BIOCHIP JOURNAL, Vol. 2, No. 3, 212-217, September 2008

Microfluidic Superparamagnetic Bead based Manipulator

Jegatha Nambi Krishnan[1], **Tae Song Kim**[1] **& Sang Kyung Kim**[1]

[1]Nano-bio Research Center, Korea Institute of Science and Technology (KIST), 39-1 Hawolgok-dong, Seongbuk-gu, Seoul 136-791, Korea
Correspondence and requests for materials should be addressed to S.K. Kim (sangk@kist.re.kr)

Accepted 14 July 2008

Abstract

This paper describes the design and fabrication of a new detection system in which the dielectrophoresis and magnetophoresis phenomena were used as a tool for the manipulation of superparamagnetic microbeads within the microchannel. By exploiting the two facts that each superparamagnetic particle exhibit different dielectrophoretic forces at different applied frequencies and do not exhibit permanent magnetic dipoles in the absence of external magnetic field, we utilized this device to perform detection of beads. We found the transition frequency range for 2.8 μm beads using our device. This device has higher trapping efficiency and less particle adsorption rate for beads. Bead based analysis revealed that high collection efficiency (~90%) could be obtained from small amount of sample solution. This high throughput detection system offers a fast analysis of magnetic beads with their velocity being maintained as 9.8 mm/s. The magnetic field distribution on the beads and the bead flow at the channel cross-section for different dielectrophoretic conditions was obtained using CFD-ACE$^+$ simulation. Our novel platform would be a useful tool in manipulating different sized superparamagnetic microbeads paving way for a multiplex detection system.

Keywords: Superparamagnetic microbeads, Dielectrophoresis (DEP), Magnetophoresis (MAP), Manipulator, Microfluidics

Introduction

In the past few years, there has been a large demand for the development of a magnetic bead-based manipulator for biochemical detection, cancer diagnostics, or drug delivery systems. Thereafter, significant efforts have been taken to transform conventional biological works into lab-on-chip by combining multiple "on-board" functions since microfluidics reduces the time and cost associated with routine analysis while improving reproducibility. Immunoassays have formed the basis for a wide array of biochemical and biological investigations[1,2]. Microbead-based assays have several advantages over the flat microarray, such as no washing steps, multiplexed assay using an encoded microbead, amplified signal due to large surface-to-volume ratio, and short assay time because of the freely moveable microbeads in mediums. An optical measurement in conjunction with bead based analysis is most commonly used for studying bead based analysis[3-5]. Such bead based analyses often include magnetic microbeads as the solid phase carrier which can bind selectively to the target to be separated. Due to the large differences in the magnetic permeabilities of the magnetic and non-magnetic materials, magnetic separation methods provide the most selective approach. Especially, superparamagnetic microbeads do not have permanent magnetic dipoles without an external magnetic field. The handling of such magnetic microbeads in lab-on-chip systems is discussed thoroughly by Gijs *et al*.[6].

Application of alternating current (AC) electrokinetic forces to control and manipulate isolated particles in suspension using microelectrode structures is a well established technique. When in a non-uniform electric field generated by electrode arrays, neutral particles exhibit a translational motion for their polarization effects. This phenomenon is so-called dielectrophoresis (DEP). DEP has been successfully used for bioparticle electrically controllable trapping, focusing, levitation, separation, translation, fractionation and characterization, and is traditionally recognized as a cell separation technique[7-11]. DEP in microelectrode systems was discussed in detail by Castellanos *et al*.[12]. Moreover, interdigitated electrode arrays have found widespread use in electrokinetics primarily for DEP separation systems wherein the DEP field is exploited to pull particles out of a fluid which continuously flow across the electrode[13]. In order to determine the ultimate limits for DEP, measurements of scaling of the DEP force with electrode size and particle size were presented by Zheng *et al*.[14]. Thus, a number of strategies have been devised to use DEP as a tool for manipulating particles in microfluidic chip. Yasukawa *et al*.[15] demonstrated the negative DEP based manipulation technique for the particles delivered at a flow rate of 1 mm/s. Gascoyne *et al*. establish-

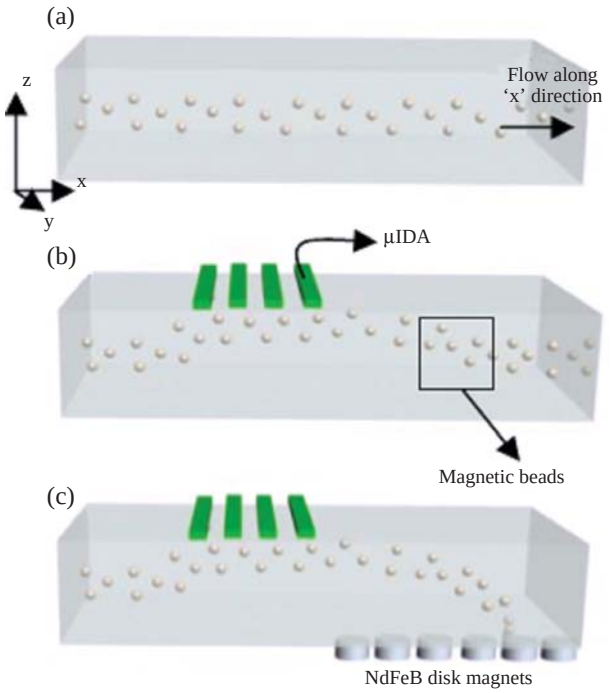

Figure 1. Shematic view of the microfluidic device (a) without μIDA and magnet, sample solution containing 2.8 μm beads achieved hydrodynamic focusing (b) with only μIDA, the beads experiencing positive DEP flow near the electrode (c) with both μIDA and magnet, the attracted beads get trapped at specific location within the microchannel.

ed the principle behind both magnetophoretic (MAP) and DEP field flow fractionation[16]. Even though electromagnets have advantages over permanent magnets in lab-on-chip systems such as their switching on/off rapidly using electrical signals, and strength of their magnetic field could be varied, still they have the disadvantage of producing weaker magnetic fields than those of permanent magnets[17]. The use of magnetics in microfluidic systems has been reviewed recently by Pamme[18-20]. Magnetophoretic immunoassay of allergen-specific IgE in an enhanced magnetic field gradient produced by the combination of the ferromagnetic microstructure with a permanent magnet was demonstrated by Hahn *et al.*[21]. The flow rate of the solution used in this system is 3 μL/h.

However, a powerful and sophisticated detection system is still required for achieving the capturing of magnetic particles at faster flow rates with high throughput. Furthermore, most lab-on-a-chip systems require low-cost magnetic bead-based manipulator integrated in them. Taking these into consideration, we have developed a new detection principle based on dielectrophoretic and magnetophoretic forces in a microfluidic channel. Particles are carried into the

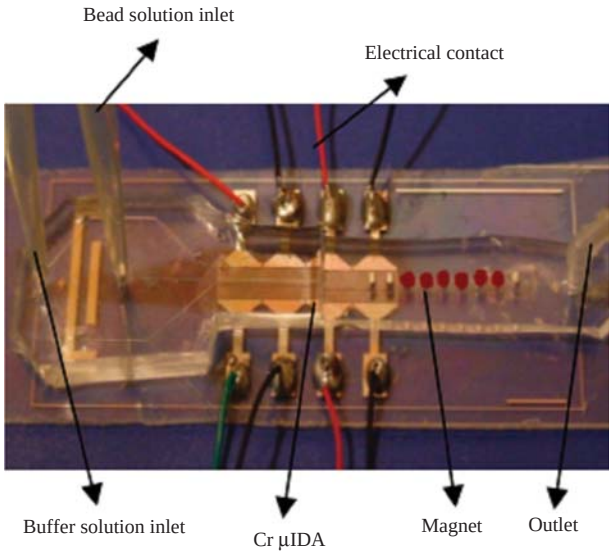

Figure 2. Experimental set up of the fully integrated device.

device as a suspension in a carrier medium that must have an appropriate conductivity, permittivity, density and viscosity. The former pair of parameters controls the DEP force and the latter pair controls the rate of sedimentation of particles. Particles are pulled out of the carrier medium onto the electrode array at a rate that depends on the frequency and flow rate[13]. Theoretically, all particles of a given size and polarisibility will collect at the same point in the device. The proposed detection scheme shown in Figure 1 is based on the fact that the superparamagnetic micro particles can be dielectrophoretically sorted, afterwhich they can only switch their path in microchannels when magnetic field induces magnetization on these beads. This assay format is especially useful to construct a multiplexed assay platform in a microfluidic device or in a lab-on-chip.

Results and Discussion

Generation of DEP Force

Figure 2 shows the integrated microfluidic platform for the manipulation of superparamagnetic beads. The bubble threshold range for both Si_3N_4 and SiO_2 insulation layer with respect to PBS was studied. A 10 V_{p-p} AC signal was applied to the system over a frequency range of 10 Hz to 1.5 MHz. The Si_3N_4 insulation layer provided wider operating window than that of SiO_2 layer. Before separating the beads, it is very essential to determine the transition frequency region for 2.8 μm beads. The flow rate during all such flow experiments was maintained to be 100 μL/min. At this con-

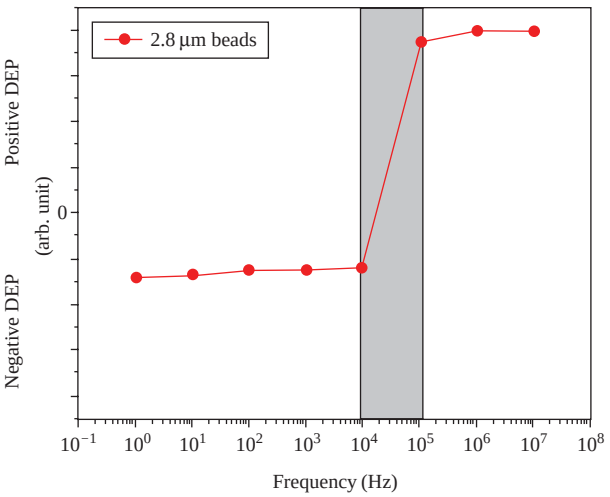

Figure 3. DEP force-frequency spectra for 2.8 µm beads-(□) cross over frequency region.

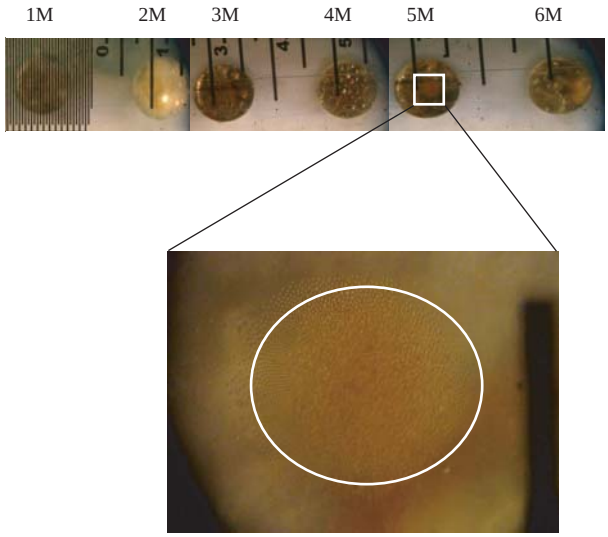

Figure 4. Trapping of the beads achieved at the fifth magnet with the experimental condition being (positive DEP) 1.3 MHz, 10 V_{p-p} and 25 µL/min where 'M' refers to the magnet.

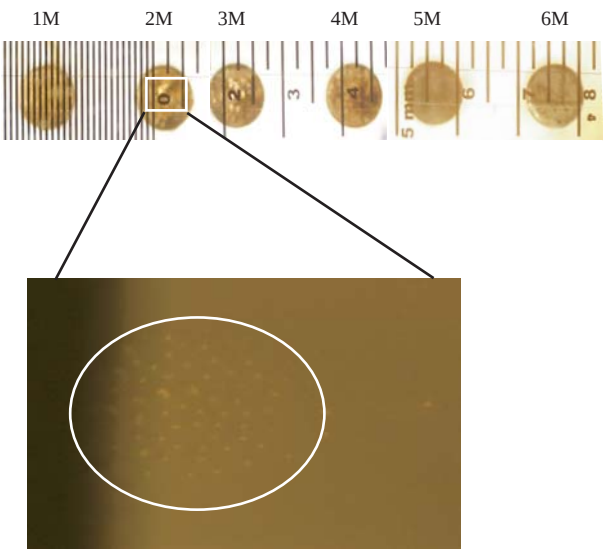

Figure 5. Trapping of the beads achieved at the second magnet with the experimental condition being (negative DEP) 50 KHz, 10 V_{p-p} and 30 µL/min where 'M' refers to the magnet.

dition, velocity of the bead at the centre of the microchannel was 39.22 mm/s. When the frequency was applied above 500 KHz at 10 V_{p-p}, the 2.8 µm beads passed through the magnets and get trapped at the farthest magnet located from the µIDA electrode. Since the beads get attracted to the µIDA electrode, they move away from getting trapped by the magnets immediate to the DEP region accounting for positive DEP. With the same flow rate, the magnetic beads got trapped at the magnets located nearer to the µIDA electrode on reducing the frequency below 500 KHz, (as they are repelled from the electrodes) thereby exhibiting negative DEP. Thus force-frequency spectra of the 2.8 µm beads was deduced by their trapping either nearer or farther of the µIDA electrodes as shown in Figure 3. Also, Green *et al*. stated that frequency-dependent DEP force is unique to a particular particle type[22]. For 2.8 µm beads, the transition frequency range was from 5 KHz (positive DEP) to 50 KHz (negative DEP). All the flow experiments include AC signal 10 V_{p-p} and flow rate of 100 µL/min with only change in applied frequency. Finally, with the help of DEP force-frequency spectra, the frequency and the flow rates were tuned to efficiently capture the beads at a specified location within the microchannel.

Detection System for Beads

From Figure 3, the applied frequencies at which 2.8 µm beads demonstrate positive and negative DEP were chosen. In order to produce positive DEP on beads, the applied frequency was fixed to be 1.3 MHz with AC signal 10 V_{p-p}. The flow experiments were carried out from 5-50 µL/min to determine the optimum flow rate at which all the beads get trapped at one location within the microchannel. The collection of beads within the microchannel was detected using the optical microscope. By adjusting the flow rate as 25 µL/min, 2.8 µm beads get trapped at the center of the 5th magnet as shown in Figure 4. At this flow rate, the velocity of the beads at the centre of the micro-

channel was 9.8 mm/s. Since the beads experience positive DEP and also the magnetic field gradient, they move away and finally get collected at the 5th magnet. Similarly, from Figure 3, DEP (50 KHz, 10 V_{p-p}) was chosen as the applied electric field for generating negative DEP on beads. When the flow rate was adjusted to be 30 µL/min, the beads got trapped at the 2nd magnet as shown in Figure 5.

Calculation of the Magnetic Field Distribution within the Detection System

We chose superparamagnetic micro beads of diameter 2.8 µm which exhibit magnetism only in the presence of external magnetic field. In our microfluidic device, the external magnetic field was applied by using six disk magnets. Since the disk magnets were placed above the microchannel, the beads flowing through the microchannel experience magnetic field depending upon their velocity profile within the microchannel.

In the developed microfluidic system, the DEP force-frequency spectra of the beads were first deduced. Then the trapping of beads were performed. In addition to this experimental approach, a numerical simulation was applied to the design of the permanent magnets and the resulting magnetic fields were investigated. The magnetic fields and forces were simulated numerically using a commercial code (CFD-ACE+, CFD Research Corporation, Huntsville, USA). In the numerical simulation process, the modules of flow, spray and magnetic fields were employed to simulate the fluid flow and magnetic field. Non-uniform adaptive mesh grids were used for numerical simulation. Also, permanent magnet source with a magnetization vector M_y=100,000 A/m was used for the calculation. These beads with diameter 2.8 µm were analyzed. From the section describing detection system for beads, it is understood that the 2.8 µm experience positive DEP and negative DEP at certain experimental conditions. In case of positive DEP, the beads get attracted to the electrode while with the negative DEP; they get repelled from the electrode[13]. Since these beads experiencing positive DEP get attracted to the electrode flow away from the top of the microchannel and the magnets too. Henceforth, we assumed that the beads experiencing the positive DEP enters from the DEP region into the MAP region at a height of 75 µm away from the top of the microchannel (Total height of the channel=85 µm). The bead flow at the channel cross-section with positive DEP conditions was obtained by CFD-ACE+, as shown in Figure 6(a). Similarly, those beads experiencing negative DEP flow along the top of the microchannel and the magnets too. Therefore, we assumed that the beads experiencing the negative DEP enters from the DEP region into the MAP region at a height of 25 µm away from the top of the microchannel. The bead flow at the channel cross-section with negative DEP conditions was obtained by CFD-ACE+, as shown in Figure 6(b). From the figures, it is crystal clear that the DEP plays a critical role in allowing the beads to enter at differ-

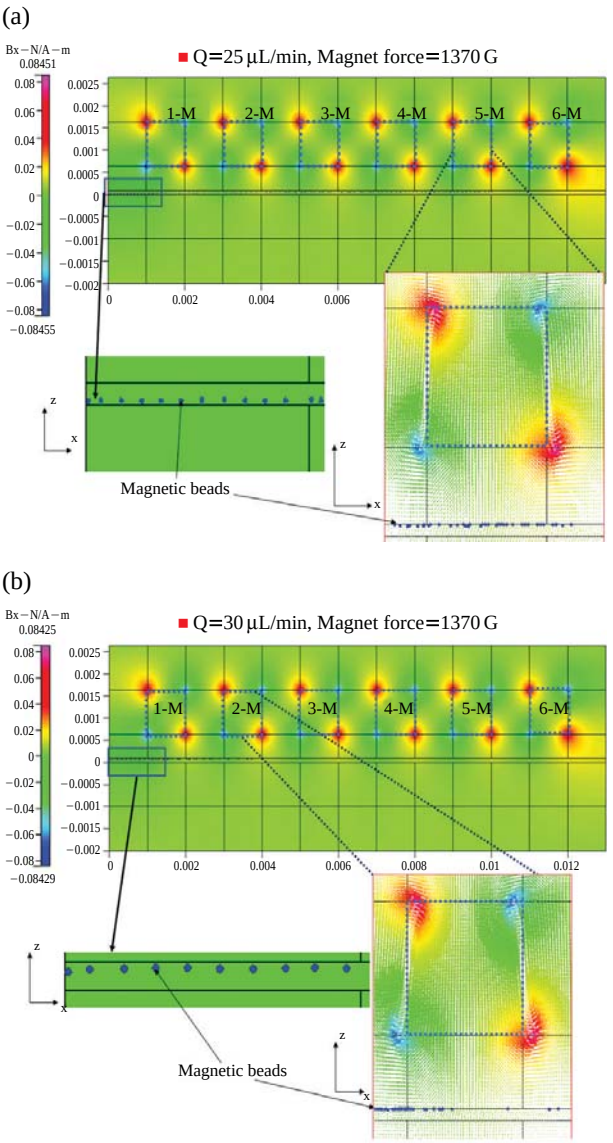

Figure 6. (a) Simulation result of the magnetic force field on 2.8 µm beads getting trapped at the 5th magnet with the flow rate of 25 µL/min (⬚) shows the magnet. The beads are assumed to flow at 75 µm away from the top of the channel due to positive DEP (1.3 MHz, 10 V_{p-p}). (b) Simulation result of the magnetic force field on 2.8 µm beads getting trapped at the 2nd magnet with the flow rate 30 µL/min. (⬚) shows the magnet. The beads are assumed to flow 25 µm away from the top of the channel due to negative DEP (50 KHz, 10 V_{p-p}).

ent heights within the microchanel. Also, the magnetic field distribution within the device locates the beads at specific sites within the microchannel. Thus, simulation and experimental results are in good agreement for this bead based microfluidic detection system.

Conclusion

We have studied the frequency response and the transition frequency range of 2.8 μm beads by using our device. The detection and collection of 2.8 μm beads using our manipulator was demonstrated. The performance of this manipulating system was verified by both experiment and simulation. The separation method proposed in this report can be used inside a microTAS device and combined upstream with bioassays and downstream with sample analysis or collection of isolated species. Such a microfluidic system enables a fast analysis with a smaller amount of reagents compared to that of the conventional method supporting its utility for analysis of disease biomarkers as well as specific allergens. This work is in progress for multiplex analysis in the real immunoassay system.

Materials and Methods

Magnetic Beads and Magnets

M-270 carboxylic acid activated Dynabeads were used for all experiments. M-270 Dynabeads are 2.8 μm in diameter and have a saturation magnetization of 13 A m^2 kg^{-1}, an initial mass susceptibility of 6.0 $\times 10^{-4}$ m^3 kg^{-1} and a density of 1.6 g DS/cm^3. The beads were suspended in the PBS solution (0.044 M NaH_2PO_4, 0.056 M Na_2HPO_4, 0.1 M KCl, 0.003 M NaN_3 1% BSA and 0.5% (v/v) Tween® 20) with a pH=7.4 to a concentration of 10^5 beads mL^{-1} where Bovine Serum albumin (BSA), sodium azide and Tween 20® were purchased from Sigma-Aldrich. All solutions were prepared using deionized water. Small, strong, permanent neodymium-iron-boron ($NdFeB^{23}$ magnets 1500 G) were used to generate a magnetic field right above the microfluidic channel. These magnets were cylindrical with a diameter of 1 mm and length 1 mm.

Device Fabrication

The polished glass wafer of thickness 1 mm was cleaned thoroughly using piranha solution. Then chromium of 300 nm thickness was deposited onto the glass wafer using the e-beam evaporator. The photoresist (PR) AZP4620 was spin coated on the Cr deposited glass wafer. The mask pattern was transferred to the PR coated wafers using soft lithography. The PR was developed using the AZ developer (CD30). After developing PR, Cr was etched using CR-7SK. Then, Cr metal electrode structure was achieved on the glass wafer. Thus, glass chips containing arrays of Cr electrode elements with equal widths and gaps of 50 μm were fabricated. By using PECVD technique, silicon nitride (Si_3N_4) or silicon dioxide (SiO_2) layer of thickness 0.5 μm was deposited. The Si_3N_4/SiO_2 layer deposited on top of the μIDA electrodes forms the insulation layer. The prepared mixture of polydimethylsiloxane (PDMS) was degassed under the vacuum, poured onto the mold and cured for 30 min at 65˚C on the hot plate. The cured PDMS was peeled from the mold. Their inlet and outlet holes were punched. The dimension of the microchannel was 85 × 500 μm. The basic plasma cleaner (PDC-32 G, Harrick plasma) was used to attach the PDMS replica onto the Si_3N_4 surface of the glass chip such that the μIDA electrode elements form the floor of the microchannel. An acryl mold was used to create space for the magnetic holders right on top of the microchannel. Six disk magnets of diameter 1 mm were placed at equal distances of 1 mm apart on those magnetic holders.

Experimental Set up and Analysis

Figure 2 shows the integrated device mounted on the inverted microscope (Olympus, Japan). The microfluidic device was composed of two inlets and one outlet. The syringe was connected with another side of tubing to pump the aqueous medium by a syringe pump (PHD 22/2000, Harvard Apparatus, Inc., MA). The buffer solution PBS (pH=7.4) flow through one of the inlets and the same solution containing the magnetic beads in the dilution ratio 1 : 1,000 v/v flow through another inlet by pulling the syringe whose tubing is connected to the outlet thereby a negative pressure is applied at the outlet. Consequently, the magnetic beads achieve hydrodynamic focusing within the microchannel. Magnetic field was applied by using the disk magnets. For the application of DEP force on the magnetic beads, a function generator (Agilent 33120A) and an oscilloscope (Agilent 54642A) were used.

Two illuminations of the microscope were used in all the experiments. The downside illumination (with high intensity) was used to create the image for virtual electrodes whereas, the upside illumination (with low intensity) was used for observation since it was difficult to see the particles in a dark region without the upside illumination. The magnetic field distribution of the disk magnets within the microfluidic channel was simulated. In order to understand these phe-

nomena more clearly, a commercial solver (CFD-ACE; CFD Research Corporation, Huntsville, AL) was used to characterize the magnetic field strength of the disk magnets.

Acknowledgements

This research has been supported by KIST grant and funding from the Intelligent Microsystem Center (IMC; http://www.microsystem.re.kr), which carries out one of the 21st century's Frontier R & D Projects sponsored by the Korea Ministry of Knowledge Economy.

References

1. Mitchell, P. Microfluidics-downsizing large-scale biology. *Nat. Biotechnol*. **19**, 717-721 (2001).
2. Microfluidic Lab-on-a-chip for Chemical and Biological Analysis and Discovery (Edited by Li, P.C.H.) Taylor & Francis Group, Boca Raton (2006).
3. Nolan, J.P. & Sklar, L.A. Suspension array technology: evolution of the flat-array paradigm. *Trends Biotechnol*. **20**, 9-12 (2002).
4. Verpoorte, E. Beads and chips: new recipes for analysis. *Lab Chip* **3**, 60-68N (2003).
5. Kim, Y.J., Kim, H.Y., Ah, C.S., Jung, M.Y. & Park, S.H. Some key factors in a bead-based fluorescence immunoassay. *Biochip J*. **2**, 60-65 (2008).
6. Gijs, M.A.M. Magnetic bead handling on-chip: new opportunities for analytical applications. *Microfluid Nanofluid* **1**, 22-40 (2004).
7. Electrical Forces on Particles (Edited by Green, N.G. & Morgan, H.) Research Studies Press Ltd., Hertfordshire (2003).
8. Yang, J., Huang, Y., Wang, X.B., Becker, F.F. & Gascoyne, P.R.C. Cell separation on microfabricated electrodes using dielectrophoretic/gravitational field flow fractionation. *Anal. Chem*. **71**, 911-918 (1999).
9. Chen, D.F., Du, H. & Li, W.H. Bioparticle separation and manipulation using dielectrophoresis. *Sens. Actuators A* **133**, 329-334 (2007).
10. Li, Y. & Kaler, K.V.I.S. Dielectrophoretic fluidic cell fractionation system. *Anal. Chim. Acta* **507**, 151-161 (2004).
11. Pommer, M.S. *et al*. Dielectrophoretic separation of platelets from diluted whole blood in microfluidic channels. *Electrophoresis* **29**, 1213-1218 (2008).
12. Castellanos, A., Ramos, A., Gonzalez, A., Green, N.G. & Morgan, H. Electrohydrodynamics and dielectrophoresis in Microsystems: scaling laws. *J. Phys. D: Appl. Phys.* **36**, 2584-2597 (2003).
13. Dielectrophoretic Separation of Sub-micrometre Particles (Edited by Green, N.G. & Morgan, H.) Research Studies Press Ltd., Hertfordshire (2003).
14. Zheng, L., Li, S., Burke, P.J. & Brody, J.P. Towards single molecule manipulation with dielectrophoresis using nanoelectrodes. *Proc. IEEE-NANO* **2**, 437-440 (2003).
15. Yasukawa, T., Suzuki, M., Sekiya, T., Shiku, H. & Matsue, T. Flow sandwich-type immunoassay in microfluidic devices based on negative dielectrophoresis. *Biosens. Bioelectron.* **22**, 2730-2736 (2007).
16. Gascoyne, P.R.C. & Vykoukal, J.V. Dielectrophoresis-based sample handling in general-purpose programmable diagnostic instruments. *Proc. IEEE* **92**, 22-42 (2004).
17. Siegel, A.C. *et al*. Cofabrication of electromagnets and microfludic systems in poly(dimethylsiloxane). *Angew. Chem. Int. Ed*. **118**, 7031-7036 (2006).
18. Pamme, N. Magnetism and microfluidics. *Lab Chip* **6**, 24-38 (2006).
19. Pamme, N. Continuous flow separations in microfluidic devices. *Lab Chip* **7**, 1644-1659 (2007).
20. Pamme, N. & Manz, A. On-chip free-flow magnetophoresis: continuous flow separation of magnetic particles and agglomerates. *Anal. Chem*. **76**, 7250-7256 (2004).
21. Hahn, Y.K. *et al*. Magnetophoretic immunoassay of allergen-specific IgE in an enhanced magnetic field gradient. *Anal. Chem.* **79**, 2214-2220 (2007).
22. Green, N.G. & Morgan, H. Separation of submicrometre particles using a combination of dielectrophoretic and electrohydrodynamic forces. *J. Phys. D: Appl. Phys.* **31**, L25-30 (1998).
23. www.mceproducts.com/knowledge-base/article/article.aspx.